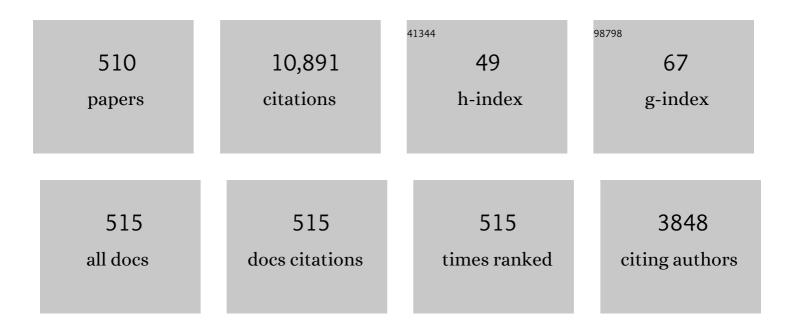
Manuel Garcia-munoz

List of Publications by Year in descending order

Source: https://exaly.com/author-pdf/3947593/publications.pdf Version: 2024-02-01



#	Article	IF	CITATIONS
1	Overview of the JET results in support to ITER. Nuclear Fusion, 2017, 57, 102001.	3.5	150
2	Major results from the first plasma campaign of the Wendelstein 7-X stellarator. Nuclear Fusion, 2017, 57, 102020.	3.5	128
3	ELM divertor peak energy fluence scaling to ITER with data from JET, MAST and ASDEX upgrade. Nuclear Materials and Energy, 2017, 12, 84-90.	1.3	116
4	Plasma wall interaction and its implication in an all tungsten divertor tokamak. Plasma Physics and Controlled Fusion, 2007, 49, B59-B70.	2.1	110
5	Magnetic configuration effects on the Wendelstein 7-X stellarator. Nature Physics, 2018, 14, 855-860.	16.7	110
6	Scintillator based detector for fast-ion losses induced by magnetohydrodynamic instabilities in the ASDEX upgrade tokamak. Review of Scientific Instruments, 2009, 80, 053503.	1.3	105
7	Isotope effects on L-H threshold and confinement in tokamak plasmas. Plasma Physics and Controlled Fusion, 2018, 60, 014045.	2.1	98
8	2D electron cyclotron emission imaging at ASDEX Upgrade (invited). Review of Scientific Instruments, 2010, 81, 10D929.	1.3	93
9	Interaction of energetic particles with large and small scale instabilities. Nuclear Fusion, 2007, 47, 025.	3.5	92
10	Power exhaust by SOL and pedestal radiation at ASDEX Upgrade and JET. Nuclear Materials and Energy, 2017, 12, 111-118.	1.3	92
11	Measurements and modeling of Alfvén eigenmode induced fast ion transport and loss in DIII-D and ASDEX Upgrade. Physics of Plasmas, 2011, 18, .	1.9	90
12	Experimental Validation of a Filament Transport Model in Turbulent Magnetized Plasmas. Physical Review Letters, 2015, 115, 215002.	7.8	89
13	Overview of the JET preparation for deuterium–tritium operation with the ITER like-wall. Nuclear Fusion, 2019, 59, 112021.	3.5	87
14	Confirmation of the topology of the Wendelstein 7-X magnetic field to better than 1:100,000. Nature Communications, 2016, 7, 13493.	12.8	85
15	Beryllium migration in JET ITER-like wall plasmas. Nuclear Fusion, 2015, 55, 063021.	3.5	83
16	WEST Physics Basis. Nuclear Fusion, 2015, 55, 063017.	3.5	82
17	Pedestal confinement and stability in JET-ILW ELMy H-modes. Nuclear Fusion, 2015, 55, 113031.	3.5	82
18	Core turbulent transport in tokamak plasmas: bridging theory and experiment with QuaLiKiz. Plasma Physics and Controlled Fusion, 2016, 58, 014036.	2.1	81

Manuel Garcia-munoz

#	Article	IF	CITATIONS
19	Energetic particle instabilities in fusion plasmas. Nuclear Fusion, 2013, 53, 104022.	3.5	79
20	Improved confinement in JET high \hat{l}^2 plasmas with an ITER-like wall. Nuclear Fusion, 2015, 55, 053031.	3.5	79
21	Efficient generation of energetic ions in multi-ion plasmas by radio-frequency heating. Nature Physics, 2017, 13, 973-978.	16.7	73
22	NTM induced fast ion losses in ASDEX Upgrade. Nuclear Fusion, 2007, 47, L10-L15.	3.5	72
23	Kinetic Alfvén eigenmodes at ASDEX Upgrade. Plasma Physics and Controlled Fusion, 2009, 51, 124009.	2.1	72
24	Overview of the JET results with the ITER-like wall. Nuclear Fusion, 2013, 53, 104002.	3.5	70
25	Fast-Ion Losses due to High-Frequency MHD Perturbations in the ASDEX Upgrade Tokamak. Physical Review Letters, 2008, 100, 055005.	7.8	68
26	Fast-ion D-alpha measurements at ASDEX Upgrade. Plasma Physics and Controlled Fusion, 2011, 53, 065010.	2.1	68
27	WALLDYN simulations of global impurity migration in JET and extrapolations to ITER. Nuclear Fusion, 2015, 55, 053015.	3.5	67
28	Fast-ion losses induced by ELMs and externally applied magnetic perturbations in the ASDEX Upgrade tokamak. Plasma Physics and Controlled Fusion, 2013, 55, 124014.	2.1	65
29	Scintillator-based diagnostic for fast ion loss measurements on DIII-D. Review of Scientific Instruments, 2010, 81, 10D307.	1.3	64
30	Stationary Zonal Flows during the Formation of the Edge Transport Barrier in the JET Tokamak. Physical Review Letters, 2016, 116, 065002.	7.8	64
31	Measurement of a 2D fast-ion velocity distribution function by tomographic inversion of fast-ion D-alpha spectra. Nuclear Fusion, 2014, 54, 023005.	3.5	62
32	Convective and Diffusive Energetic Particle Losses Induced by Shear Alfvén Waves in the ASDEX Upgrade Tokamak. Physical Review Letters, 2010, 104, 185002.	7.8	61
33	Dual sightline measurements of MeV range deuterons with neutron and gamma-ray spectroscopy at JET. Nuclear Fusion, 2015, 55, 123026.	3.5	60
34	Tomography of fast-ion velocity-space distributions from synthetic CTS and FIDA measurements. Nuclear Fusion, 2012, 52, 103008.	3.5	59
35	Runaway electron beam generation and mitigation during disruptions at JET-ILW. Nuclear Fusion, 2015, 55, 093013.	3.5	58
36	Melt damage to the JET ITER-like Wall and divertor. Physica Scripta, 2016, T167, 014070.	2.5	58

#	Article	IF	CITATIONS
37	Erosion and deposition in the JET divertor during the first ILW campaign. Physica Scripta, 2016, T167, 014051.	2.5	58
38	Tractable flux-driven temperature, density, and rotation profile evolution with the quasilinear gyrokinetic transport model QuaLiKiz. Plasma Physics and Controlled Fusion, 2017, 59, 124005.	2.1	57
39	Correlation of the tokamak H-mode density limit with ballooning stability at the separatrix. Nuclear Fusion, 2018, 58, 034001.	3.5	57
40	Key impact of finite-beta and fast ions in core and edge tokamak regions for the transition to advanced scenarios. Nuclear Fusion, 2015, 55, 053007.	3.5	56
41	Influence of theE  ×  Bdrift in high recycling divertors on target asymmetries. Plasma Physics a Controlled Fusion, 2015, 57, 095002.	ind 2.1	56
42	Recent progress towards a quantitative description of filamentary SOL transport. Nuclear Fusion, 2017, 57, 056044.	3.5	56
43	Overview of ASDEX Upgrade results. Nuclear Fusion, 2017, 57, 102015.	3.5	53
44	Fast-ion transport induced by Alfvén eigenmodes in the ASDEX Upgrade tokamak. Nuclear Fusion, 2011, 51, 103013.	3.5	52
45	Long-term fuel retention in JET ITER-like wall. Physica Scripta, 2016, T167, 014075.	2.5	52
46	MeV-range velocity-space tomography from gamma-ray and neutron emission spectrometry measurements at JET. Nuclear Fusion, 2017, 57, 056001.	3.5	52
47	Dust generation in tokamaks: Overview of beryllium and tungsten dust characterisation in JET with the ITER-like wall. Fusion Engineering and Design, 2018, 136, 579-586.	1.9	52
48	First dust study in JET with the ITER-like wall: sampling, analysis and classification. Nuclear Fusion, 2015, 55, 113033.	3.5	51
49	Scaling of the MHD perturbation amplitude required to trigger a disruption and predictions for ITER. Nuclear Fusion, 2016, 56, 026007.	3.5	51
50	Overview of the JET results. Nuclear Fusion, 2015, 55, 104001.	3.5	50
51	Recent progress in fast-ion diagnostics for magnetically confined plasmas. Reviews of Modern Plasma Physics, 2018, 2, 1.	4.1	50
52	The impact of poloidal asymmetries on tungsten transport in the core of JET H-mode plasmas. Physics of Plasmas, 2015, 22, 055902.	1.9	49
53	Characterization of off-axis fishbones. Plasma Physics and Controlled Fusion, 2011, 53, 085028.	2.1	48
54	Fast-ion redistribution and loss due to edge perturbations in the ASDEX Upgrade, DIII-D and KSTAR tokamaks. Nuclear Fusion, 2013, 53, 123008.	3.5	47

#	Article	IF	CITATIONS
55	Electron cyclotron heating can drastically alter reversed shear Alfvén eigenmode activity in DIII-D through finite pressure effects. Nuclear Fusion, 2016, 56, 112007.	3.5	47
56	Progress in understanding disruptions triggered by massive gas injection via 3D non-linear MHD modelling with JOREK. Plasma Physics and Controlled Fusion, 2017, 59, 014006.	2.1	47
57	Overview of fuel inventory in JET with the ITER-like wall. Nuclear Fusion, 2017, 57, 086045.	3.5	47
58	Overview of JET results. Nuclear Fusion, 2009, 49, 104006.	3.5	46
59	Overview of the JET ITER-like wall divertor. Nuclear Materials and Energy, 2017, 12, 499-505.	1.3	46
60	Observation and modelling of fast ion loss in JET and ASDEX Upgrade. Nuclear Fusion, 2006, 46, S904-S910.	3.5	45
61	Combination of fast-ion diagnostics in velocity-space tomographies. Nuclear Fusion, 2013, 53, 063019.	3.5	45
62	Three-dimensional non-linear magnetohydrodynamic modeling of massive gas injection triggered disruptions in JET. Physics of Plasmas, 2015, 22, .	1.9	45
63	Ion target impact energy during Type I edge localized modes in JET ITER-like Wall. Plasma Physics and Controlled Fusion, 2015, 57, 085006.	2.1	44
64	Adaptive predictors based on probabilistic SVM for real time disruption mitigation on JET. Nuclear Fusion, 2018, 58, 056002.	3.5	44
65	MHD induced fast-ion losses on ASDEX Upgrade. Nuclear Fusion, 2009, 49, 085014.	3.5	43
66	Alfvén eigenmode stability and fast ion loss in DIII-D and ITER reversed magnetic shear plasmas. Nuclear Fusion, 2012, 52, 094023.	3.5	43
67	Real-time control of divertor detachment in H-mode with impurity seeding using Langmuir probe feedback in JET-ITER-like wall. Plasma Physics and Controlled Fusion, 2017, 59, 045001.	2.1	43
68	Physics research on the TCV tokamak facility: from conventional to alternative scenarios and beyond. Nuclear Fusion, 2019, 59, 112023.	3.5	43
69	Fast ion transport during applied 3D magnetic perturbations on DIII-D. Nuclear Fusion, 2015, 55, 073028.	3.5	42
70	First neutron spectroscopy measurements with a pixelated diamond detector at JET. Review of Scientific Instruments, 2016, 87, 11D833.	1.3	42
71	Physics and applications of three-ion ICRF scenarios for fusion research. Physics of Plasmas, 2021, 28, .	1.9	42
72	Observation and modeling of fast trapped ion losses due to neoclassical tearing modes. Physics of Plasmas, 2008, 15, .	1.9	41

#	Article	IF	CITATIONS
73	Studies of dust from JET with the ITER-Like Wall: Composition and internal structure. Nuclear Materials and Energy, 2017, 12, 582-587.	1.3	41
74	Real-time-capable prediction of temperature and density profiles in a tokamak using RAPTOR and a first-principle-based transport model. Nuclear Fusion, 2018, 58, 096006.	3.5	41
75	Inferring divertor plasma properties from hydrogen Balmer and Paschen series spectroscopy in JET-ILW. Nuclear Fusion, 2015, 55, 123028.	3.5	40
76	Toroidal modelling of resonant magnetic perturbations response in ASDEX-Upgrade: coupling between field pitch aligned response and kink amplification. Plasma Physics and Controlled Fusion, 2015, 57, 095008.	2.1	40
77	JET and COMPASS asymmetrical disruptions. Nuclear Fusion, 2015, 55, 113006.	3.5	40
78	Phase-space resolved measurement of 2nd harmonic ion cyclotron heating using FIDA tomography at the ASDEX Upgrade tokamak. Nuclear Fusion, 2017, 57, 116058.	3.5	40
79	Integrated modelling of H-mode pedestal and confinement in JET-ILW. Plasma Physics and Controlled Fusion, 2018, 60, 014042.	2.1	40
80	Application of Gaussian process regression to plasma turbulent transport model validation via integrated modelling. Nuclear Fusion, 2019, 59, 056007.	3.5	39
81	Overview of JET results. Nuclear Fusion, 2003, 43, 1540-1554.	3.5	38
82	Investigation into the formation of the scrape-off layer density shoulder in JET ITER-like wall L-mode and H-mode plasmas. Nuclear Fusion, 2018, 58, 056001.	3.5	38
83	Effect of the relative shift between the electron density and temperature pedestal position on the pedestal stability in JET-ILW and comparison with JET-C. Nuclear Fusion, 2018, 58, 056010.	3.5	38
84	Overview of physics studies on ASDEX Upgrade. Nuclear Fusion, 2019, 59, 112014.	3.5	38
85	Physics of Plasmas, 2015, 22, 056115.	1.9	37
86	The role of MHD in causing impurity peaking in JET hybrid plasmas. Nuclear Fusion, 2016, 56, 066002.	3.5	37
87	Active control of Alfvén eigenmodes in magnetically confined toroidal plasmas. Plasma Physics and Controlled Fusion, 2019, 61, 054007.	2.1	37
88	Overview of ASDEX Upgrade results. Nuclear Fusion, 2013, 53, 104003.	3.5	36
89	Modulation of prompt fast-ion loss by applied <i>n</i> = 2 fields in the DIII-D tokamak. Plasma Physics and Controlled Fusion, 2014, 56, 015009.	2.1	36
90	Multi-machine scaling of the main SOL parallel heat flux width in tokamak limiter plasmas. Plasma Physics and Controlled Fusion, 2016, 58, 074005.	2.1	36

#	Article	IF	CITATIONS
91	Understanding the physics of ELM pacing via vertical kicks in JET in view of ITER. Nuclear Fusion, 2016, 56, 026001.	3.5	36
92	Neutron spectroscopy measurements of 14 MeV neutrons at unprecedented energy resolution and implications for deuterium–tritium fusion plasma diagnostics. Measurement Science and Technology, 2018, 29, 045502.	2.6	35
93	Observations of core ion cyclotron emission on ASDEX Upgrade tokamak. Review of Scientific Instruments, 2018, 89, 10/101.	1.3	35
94	Deep learning for plasma tomography using the bolometer system at JET. Fusion Engineering and Design, 2017, 114, 18-25.	1.9	34
95	Dynamics and stability of divertor detachment in H-mode plasmas on JET. Plasma Physics and Controlled Fusion, 2017, 59, 095003.	2.1	34
96	Scenario development for the observation of alpha-driven instabilities in JET DT plasmas. Nuclear Fusion, 2018, 58, 082005.	3.5	34
97	Dependence on plasma shape and plasma fueling for small edge-localized mode regimes in TCV and ASDEX Upgrade. Nuclear Fusion, 2019, 59, 086020.	3.5	34
98	Overview of JET results. Nuclear Fusion, 2011, 51, 094008.	3.5	33
99	Discriminating the trapped electron modes contribution in density fluctuation spectra. Nuclear Fusion, 2015, 55, 093021.	3.5	33
100	Transport analysis and modelling of the evolution of hollow density profiles plasmas in JET and implication for ITER. Nuclear Fusion, 2015, 55, 123001.	3.5	33
101	Challenges in the extrapolation from DD to DT plasmas: experimental analysis and theory based predictions for JET-DT. Plasma Physics and Controlled Fusion, 2017, 59, 014023.	2.1	33
102	Velocity-space sensitivity and tomography of scintillator-based fast-ion loss detectors. Plasma Physics and Controlled Fusion, 2018, 60, 105005.	2.1	33
103	Fast H isotope and impurity mixing in ion-temperature-gradient turbulence. Nuclear Fusion, 2018, 58, 076028.	3.5	33
104	Ion cyclotron resonance heating for tungsten control in various JET H-mode scenarios. Plasma Physics and Controlled Fusion, 2017, 59, 055001.	2.1	32
105	Experimental estimation of tungsten impurity sputtering due to Type I ELMs in JET-ITER-like wall using pedestal electron cyclotron emission and target Langmuir probe measurements. Physica Scripta, 2016, T167, 014005.	2.5	31
106	Gamma-ray spectroscopy at MHz counting rates with a compact LaBr3 detector and silicon photomultipliers for fusion plasma applications. Review of Scientific Instruments, 2016, 87, 11E714.	1.3	31
107	Fast-ion energy resolution by one-step reaction gamma-ray spectrometry. Nuclear Fusion, 2016, 56, 046009.	3.5	31
108	A First Analysis of JET Plasma Profile-Based Indicators for Disruption Prediction and Avoidance. IEEE Transactions on Plasma Science, 2018, 46, 2691-2698.	1.3	31

#	Article	IF	CITATIONS
109	Validation of the ICRF antenna coupling code RAPLICASOL against TOPICA and experiments. Nuclear Fusion, 2019, 59, 046001.	3.5	31
110	Structure and dynamics of spontaneous and induced ELMs on ASDEX Upgrade. Nuclear Fusion, 2008, 48, 045005.	3.5	30
111	Multi-view fast-ion D-alpha spectroscopy diagnostic at ASDEX Upgrade. Review of Scientific Instruments, 2013, 84, 113502.	1.3	30
112	Cell Assembly Signatures Defined by Short-Term Synaptic Plasticity in Cortical Networks. International Journal of Neural Systems, 2015, 25, 1550026.	5.2	30
113	Velocity-space sensitivities of neutron emission spectrometers at the tokamaks JET and ASDEX Upgrade in deuterium plasmas. Review of Scientific Instruments, 2017, 88, 073506.	1.3	30
114	Studies of the pedestal structure and inter-ELM pedestal evolution in JET with the ITER-like wall. Nuclear Fusion, 2017, 57, 116012.	3.5	30
115	Characterisation of the fast-ion edge resonant transport layer induced by 3D perturbative fields in the ASDEX Upgrade tokamak through full orbit simulations. Plasma Physics and Controlled Fusion, 2019, 61, 014038.	2.1	30
116	Overview of the TCV tokamak experimental programme. Nuclear Fusion, 2022, 62, 042018.	3.5	30
117	Initial measurements of fast ion loss in KSTAR. Review of Scientific Instruments, 2012, 83, 10D305.	1.3	29
118	Benchmark experiments on neutron streaming through JET Torus Hall penetrations. Nuclear Fusion, 2015, 55, 053028.	3.5	29
119	Axisymmetric oscillations at L–H transitions in JET: M-mode. Nuclear Fusion, 2017, 57, 022021.	3.5	29
120	Non-Maxwellian fast particle effects in gyrokinetic GENE simulations. Physics of Plasmas, 2018, 25, .	1.9	29
121	3D non-linear MHD simulation of the MHD response and density increase as a result of shattered pellet injection. Nuclear Fusion, 2018, 58, 126025.	3.5	29
122	Modelling of JET hybrid plasmas with emphasis on performance of combined ICRF and NBI heating. Nuclear Fusion, 2018, 58, 106037.	3.5	29
123	Overview of ASDEX Upgrade results—development of integrated operating scenarios for ITER. Nuclear Fusion, 2005, 45, S98-S108.	3.5	28
124	Plasma confinement at JET. Plasma Physics and Controlled Fusion, 2016, 58, 014034.	2.1	28
125	Assessment of erosion, deposition and fuel retention in the JET-ILW divertor from ion beam analysis data. Nuclear Materials and Energy, 2017, 12, 559-563.	1.3	28
126	Overview of ASDEX Upgrade results. Nuclear Fusion, 2011, 51, 094012.	3.5	27

#	Article	IF	CITATIONS
127	Characterisation of the deuterium recycling at the W divertor target plates in JET during steady-state plasma conditions and ELMs. Physica Scripta, 2016, T167, 014076.	2.5	27
128	Gyrokinetic study of turbulent convection of heavy impurities in tokamak plasmas at comparable ion and electron heat fluxes. Nuclear Fusion, 2017, 57, 022009.	3.5	27
129	Assessment of SOLPS5.0 divertor solutions with drifts and currents against L-mode experiments in ASDEX Upgrade and JET. Plasma Physics and Controlled Fusion, 2017, 59, 035003.	2.1	27
130	First ERO2.0 modeling of Be erosion and non-local transport in JET ITER-like wall. Physica Scripta, 2017, T170, 014018.	2.5	27
131	Erosion and deposition in the JET divertor during the second ITER-like wall campaign. Physica Scripta, 2017, T170, 014058.	2.5	27
132	NBI-driven Alfvénic modes at ASDEX Upgrade. Nuclear Fusion, 2012, 52, 094007.	3.5	26
133	Influence of externally applied magnetic perturbations on neoclassical tearing modes at ASDEX Upgrade. Nuclear Fusion, 2015, 55, 013018.	3.5	26
134	An Analytical Expression for the Electric Field and Particle Tracing in Modelling of Be Erosion Experiments at the JET ITERâ€like Wall. Contributions To Plasma Physics, 2016, 56, 640-645.	1.1	26
135	Technological exploitation of Deuterium–Tritium operations at JET in support of ITER design, operation and safety. Fusion Engineering and Design, 2016, 109-111, 278-285.	1.9	26
136	Experience on divertor fuel retention after two ITER-Like Wall campaigns. Physica Scripta, 2017, T170, 014063.	2.5	26
137	Dimensionless scalings of confinement, heat transport and pedestal stability in JET-ILW and comparison with JET-C. Plasma Physics and Controlled Fusion, 2017, 59, 014014.	2.1	26
138	Test particles dynamics in the JOREK 3D non-linear MHD code and application to electron transport in a disruption simulation. Nuclear Fusion, 2018, 58, 016043.	3.5	26
139	The effects of electron cyclotron heating and current drive on toroidal Alfvén eigenmodes in tokamak plasmas. Plasma Physics and Controlled Fusion, 2018, 60, 014026.	2.1	26
140	Assessment of the baseline scenario at <i>q</i> ₉₅ ~ 3 for ITER. Nuclear Fusion, 2018, 58, 126010.	3.5	26
141	W transport and accumulation control in the termination phase of JET H-mode discharges and implications for ITER. Plasma Physics and Controlled Fusion, 2018, 60, 074008.	2.1	26
142	Runaway electron beam control. Plasma Physics and Controlled Fusion, 2019, 61, 014036.	2.1	26
143	A flexible luminescent probe to monitor fast ion losses at the edge of the TJ-II stellarator. Review of Scientific Instruments, 2008, 79, 093511.	1.3	25
144	Convective beam ion losses due to Alfvén eigenmodes in DIII-D reversed-shear plasmas. Plasma Physics and Controlled Fusion, 2011, 53, 062001.	2.1	25

#	Article	IF	CITATIONS
145	Investigation of fast particle driven instabilities by 2D electron cyclotron emission imaging on ASDEX Upgrade. Plasma Physics and Controlled Fusion, 2011, 53, 124018.	2.1	25
146	Simulations of fast ion wall loads in ASDEX Upgrade in the presence of magnetic perturbations due to ELM-mitigation coils. Nuclear Fusion, 2012, 52, 094014.	3.5	25
147	Fast-ion transport in the presence of magnetic reconnection induced by sawtooth oscillations in ASDEX Upgrade. Nuclear Fusion, 2014, 54, 022005.	3.5	25
148	Fast ion energy distribution from third harmonic radio frequency heating measured with a single crystal diamond detector at the Joint European Torus. Review of Scientific Instruments, 2015, 86, 103501.	1.3	25
149	Impact of divertor geometry on radiative divertor performance in JET H-mode plasmas. Plasma Physics and Controlled Fusion, 2016, 58, 045011.	2.1	25
150	Plasma impact on diagnostic mirrors in JET. Nuclear Materials and Energy, 2017, 12, 506-512.	1.3	25
151	Recent progress in the quantitative validation of JOREK simulations of ELMs in JET. Nuclear Fusion, 2017, 57, 076006.	3.5	25
152	Fuel inventory and deposition in castellated structures in JET-ILW. Nuclear Fusion, 2017, 57, 066027.	3.5	25
153	Long-term fuel retention and release in JET ITER-Like Wall at ITER-relevant baking temperatures. Nuclear Fusion, 2017, 57, 086024.	3.5	25
154	Maximum likelihood bolometric tomography for the determination of the uncertainties in the radiation emission on JET TOKAMAK. Review of Scientific Instruments, 2018, 89, 053504.	1.3	25
155	Material migration and fuel retention studies during the JET carbon divertor campaigns. Fusion Engineering and Design, 2019, 138, 78-108.	1.9	25
156	The †̃neutron deficit' in the JET tokamak. Nuclear Fusion, 2017, 57, 076029.	3.5	25
157	Performance of the prototype LaBr3 spectrometer developed for the JET gamma-ray camera upgrade. Review of Scientific Instruments, 2016, 87, 11E717.	1.3	24
158	Experimental investigation of geodesic acoustic modes on JET using Doppler backscattering. Nuclear Fusion, 2016, 56, 106026.	3.5	24
159	Impact of divertor geometry on H-mode confinement in the JET metallic wall. Nuclear Fusion, 2017, 57, 086025.	3.5	24
160	Collective Thomson scattering measurements of fast-ion transport due to sawtooth crashes in ASDEX Upgrade. Nuclear Fusion, 2016, 56, 112014.	3.5	23
161	Asymmetric toroidal eddy currents (ATEC) to explain sideways forces at JET. Nuclear Fusion, 2016, 56, 106010.	3.5	23
162	Overview of progress in European medium sized tokamaks towards an integrated plasma-edge/wall solution ^a . Nuclear Fusion, 2017, 57, 102014.	3.5	23

#	Article	IF	CITATIONS
163	Sawtooth pacing with on-axis ICRH modulation in JET-ILW. Nuclear Fusion, 2017, 57, 036027.	3.5	23
164	High fusion performance at high <i>T</i> _i / <i>T</i> _e in JET-ILW baseline plasmas with high NBI heating power and low gas puffing. Nuclear Fusion, 2018, 58, 036020.	3.5	23
165	Instrumentation for the upgrade to the JET core charge-exchange spectrometers. Review of Scientific Instruments, 2018, 89, 10D113.	1.3	23
166	Impact of electron-scale turbulence and multi-scale interactions in the JET tokamak. Nuclear Fusion, 2018, 58, 124003.	3.5	23
167	Measuring fast ions in fusion plasmas with neutron diagnostics at JET. Plasma Physics and Controlled Fusion, 2019, 61, 014027.	2.1	23
168	Determination of isotope ratio in the divertor of JET-ILW by high-resolution H <i>α</i> spectroscopy: H–D experiment and implications for D–T experiment. Nuclear Fusion, 2019, 59, 046011.	3.5	23
169	Determination of tungsten and molybdenum concentrations from an x-ray range spectrum in JET with the ITER-like wall configuration. Journal of Physics B: Atomic, Molecular and Optical Physics, 2015, 48, 144023.	1.5	22
170	Gyrokinetic study of turbulence suppression in a JET-ILW power scan. Plasma Physics and Controlled Fusion, 2016, 58, 115005.	2.1	22
171	Neutron emission spectroscopy of DT plasmas at enhanced energy resolution with diamond detectors. Review of Scientific Instruments, 2016, 87, 11D822.	1.3	22
172	Global and pedestal confinement and pedestal structure in dimensionless collisionality scans of low-triangularity H-mode plasmas in JET-ILW. Nuclear Fusion, 2017, 57, 016012.	3.5	22
173	Modelling of transitions between L- and H-mode in JET high plasma current plasmas and application to ITER scenarios including tungsten behaviour. Nuclear Fusion, 2017, 57, 086023.	3.5	22
174	Fine metal dust particles on the wall probes from JET-ILW. Physica Scripta, 2017, T170, 014038.	2.5	22
175	Full-Pulse Tomographic Reconstruction with Deep Neural Networks. Fusion Science and Technology, 2018, 74, 47-56.	1.1	22
176	14 MeV calibration of JET neutron detectors—phase 1: calibration and characterization of the neutron source. Nuclear Fusion, 2018, 58, 026012.	3.5	22
177	First principles of modelling the stabilization of microturbulence by fast ions. Nuclear Fusion, 2018, 58, 082024.	3.5	22
178	First principle integrated modeling of multi-channel transport including Tungsten in JET. Nuclear Fusion, 2018, 58, 096003.	3.5	22
179	Evolution of nitrogen concentration and ammonia production in N ₂ -seeded H-mode discharges at ASDEX Upgrade. Nuclear Fusion, 2019, 59, 046010.	3.5	22
180	Numerical simulations of fast ion loss measurements induced by magnetic islands in the ASDEX Upgrade tokamak. Nuclear Fusion, 2009, 49, 095021.	3.5	21

Manuel Garcia-munoz

#	Article	IF	CITATIONS
181	Radiation asymmetries during the thermal quench of massive gas injection disruptions in JET. Nuclear Fusion, 2015, 55, 123027.	3.5	21
182	Experimental evaluation of stable long term operation of semiconductor magnetic sensors at ITER relevant environment. Nuclear Fusion, 2015, 55, 083006.	3.5	21
183	The upgraded JET gamma-ray cameras based on high resolution/high count rate compact spectrometers. Review of Scientific Instruments, 2018, 89, 101116.	1.3	21
184	Electron acceleration in a JET disruption simulation. Nuclear Fusion, 2018, 58, 106022.	3.5	21
185	ICRF physics aspects of wall conditioning with conventional antennas in large-size tokamaks. Journal of Nuclear Materials, 2011, 415, S1029-S1032.	2.7	20
186	Near midplane scintillator-based fast ion loss detector on DIII-D. Review of Scientific Instruments, 2012, 83, 10D707.	1.3	20
187	Non-linear MHD simulations of ELMs in JET and quantitative comparisons to experiments. Plasma Physics and Controlled Fusion, 2016, 58, 014026.	2.1	20
188	Deuterium trapping and release in JET ITER-like wall divertor tiles. Physica Scripta, 2016, T167, 014074.	2.5	20
189	ITER oriented neutronics benchmark experiments on neutron streaming and shutdown dose rate at JET. Fusion Engineering and Design, 2017, 123, 171-176.	1.9	20
190	Simulation of neutral gas flow in the JET sub-divertor. Fusion Engineering and Design, 2017, 121, 13-21.	1.9	20
191	Transient induced tungsten melting at the Joint European Torus (JET). Physica Scripta, 2017, T170, 014013.	2.5	20
192	Physics and operation oriented activities in preparation of the JT-60SA tokamak exploitation. Nuclear Fusion, 2017, 57, 085001.	3.5	20
193	Multi-machine analysis of termination scenarios with comparison to simulations of controlled shutdown of ITER discharges. Nuclear Fusion, 2018, 58, 026019.	3.5	20
194	Experimental validation of an analytical kinetic model for edge-localized modes in JET-ITER-like wall. Nuclear Fusion, 2018, 58, 066006.	3.5	20
195	Identification of BeO and BeOxDy in melted zones of the JET Be limiter tiles: Raman study using comparison with laboratory samples. Nuclear Materials and Energy, 2018, 17, 295-301.	1.3	20
196	Tritium retention characteristics in dust particles in JET with ITER-like wall. Nuclear Materials and Energy, 2018, 17, 279-283.	1.3	20
197	Equilibrium reconstruction at JET using Stokes model for polarimetry. Nuclear Fusion, 2018, 58, 106032.	3.5	20
198	Observation of enhanced ion particle transport in mixed H/D isotope plasmas on JET. Nuclear Fusion, 2018, 58, 076022.	3.5	20

#	Article	IF	CITATIONS
199	14 MeV calibration of JET neutron detectors—phase 2: in-vessel calibration. Nuclear Fusion, 2018, 58, 106016.	3.5	20
200	Modeling the response of a fast ion loss detector using orbit tracing techniques in a neutral beam prompt-loss study on the DIII-D tokamak. Review of Scientific Instruments, 2010, 81, 10D305.	1.3	19
201	Gamma-ray spectroscopy measurements of confined fast ions on ASDEX Upgrade. Nuclear Fusion, 2012, 52, 094021.	3.5	19
202	Neutronics experiments and analyses in preparation of DT operations at JET. Fusion Engineering and Design, 2016, 109-111, 895-905.	1.9	19
203	JET experiments with tritium and deuterium–tritium mixtures. Fusion Engineering and Design, 2016, 109-111, 925-936.	1.9	19
204	Impact of toroidal and poloidal mode spectra on the control of non-axisymmetric fields in tokamaks. Physics of Plasmas, 2017, 24, .	1.9	19
205	Mitigation of divertor heat loads by strike point sweeping in high power JET discharges. Physica Scripta, 2017, T170, 014040.	2.5	19
206	Neutral pathways and heat flux widths in vertical- and horizontal-target EDGE2D-EIRENE simulations of JET. Nuclear Fusion, 2018, 58, 096029.	3.5	19
207	Thermal desorption spectrometry of beryllium plasma facing tiles exposed in the JET tokamak. Fusion Engineering and Design, 2018, 133, 135-141.	1.9	19
208	Fast-ion losses induced by ACs and TAEs in the ASDEX Upgrade tokamak. Nuclear Fusion, 2010, 50, 084004.	3.5	18
209	Beam ion losses due to energetic particle geodesic acoustic modes. Nuclear Fusion, 2012, 52, 123015.	3.5	18
210	Multi-mode Alfvénic fast particle transport and losses: numerical versus experimental observation. Nuclear Fusion, 2013, 53, 123003.	3.5	18
211	L to H mode transition: parametric dependencies of the temperature threshold. Nuclear Fusion, 2015, 55, 073015.	3.5	18
212	High performance detectors for upgraded gamma ray diagnostics for JET DT campaigns. Physica Scripta, 2016, 91, 064003.	2.5	18
213	Response function of single crystal synthetic diamond detectors to 1-4 MeV neutrons for spectroscopy of D plasmas. Review of Scientific Instruments, 2016, 87, 11D823.	1.3	18
214	Nitrogen retention mechanisms in tokamaks with beryllium and tungsten plasma-facing surfaces. Physica Scripta, 2016, T167, 014077.	2.5	18
215	Experience of handling beryllium, tritium and activated components from JET ITER like wall. Physica Scripta, 2016, T167, 014057.	2.5	18
216	The role and application of ion beam analysis for studies of plasma-facing components in controlled fusion devices. Nuclear Instruments & Methods in Physics Research B, 2016, 371, 4-11.	1.4	18

#	Article	IF	CITATIONS
217	Application of transfer entropy to causality detection and synchronization experiments in tokamaks. Nuclear Fusion, 2016, 56, 026006.	3.5	18
218	Energy balance in JET. Nuclear Materials and Energy, 2017, 12, 227-233.	1.3	18
219	A multi-machine scaling of halo current rotation. Nuclear Fusion, 2018, 58, 016050.	3.5	18
220	Analysis of deposited layers with deuterium and impurity elements on samples from the divertor of JET with ITER-like wall. Journal of Nuclear Materials, 2019, 516, 202-213.	2.7	18
221	Advances in the physics studies for the JT-60SA tokamak exploitation and research plan. Plasma Physics and Controlled Fusion, 2020, 62, 014009.	2.1	18
222	MeV-range fast ion losses induced by fishbones on JET. Nuclear Fusion, 2010, 50, 084009.	3.5	17
223	Solitary magnetic perturbations at the ELM onset. Nuclear Fusion, 2012, 52, 114025.	3.5	17
224	Benchmarking the GENE and GYRO codes through the relative roles of electromagnetic and <i>E</i> — <i>B</i> stabilization in JET high-performance discharges. Plasma Physics and G Fusion, 2016, 58, 125018.	2 en trolled	17
225	Improved ERO modelling for spectroscopy of physically and chemically assisted eroded beryllium from the JET-ILW. Nuclear Materials and Energy, 2016, 9, 604-609.	1.3	17
226	Plasma edge and plasma-wall interaction modelling: Lessons learned from metallic devices. Nuclear Materials and Energy, 2017, 12, 3-17.	1.3	17
227	Investigation and plasma cleaning of first mirrors coated with relevant ITER contaminants: beryllium and tungsten. Nuclear Fusion, 2017, 57, 086019.	3.5	17
228	Calibration of neutron detectors on the Joint European Torus. Review of Scientific Instruments, 2017, 88, 103505.	1.3	17
229	Versatile fusion source integrator AFSI for fast ion and neutron studies in fusion devices. Nuclear Fusion, 2018, 58, 016023.	3.5	17
230	Velocity space resolved absolute measurement of fast ion losses induced by a tearing mode in the ASDEX Upgrade tokamak. Nuclear Fusion, 2018, 58, 036005.	3.5	17
231	High-resolution tungsten spectroscopy relevant to the diagnostic of high-temperature tokamak plasmas. Physical Review A, 2018, 97, .	2.5	17
232	Analysis of ELM stability with extended MHD models in JET, JT-60U and future JT-60SA tokamak plasmas. Plasma Physics and Controlled Fusion, 2018, 60, 014032.	2.1	17
233	Effects of nitrogen seeding on core ion thermal transport in JET ILW L-mode plasmas. Nuclear Fusion, 2018, 58, 026028.	3.5	17
234	Synthetic spectra of BeH, BeD and BeT for emission modeling in JET plasmas. Journal of Physics B: Atomic, Molecular and Optical Physics, 2018, 51, 185701.	1.5	17

#	Article	IF	CITATIONS
235	Activation of ITER materials in JET: nuclear characterisation experiments for the long-term irradiation station. Nuclear Fusion, 2018, 58, 096013.	3.5	17
236	Recent ASDEX Upgrade research in support of ITER and DEMO. Nuclear Fusion, 2015, 55, 104010.	3.5	16
237	Conceptual design of the ITER fast-ion loss detector. Review of Scientific Instruments, 2016, 87, 11D829.	1.3	16
238	Possible influence of near SOL plasma on the H-mode power threshold. Nuclear Materials and Energy, 2017, 12, 273-277.	1.3	16
239	Axisymmetric global Alfvén eigenmodes within the ellipticity-induced frequency gap in the Joint European Torus. Physics of Plasmas, 2017, 24, .	1.9	16
240	Bayesian electron density inference from JET lithium beam emission spectra using Gaussian processes. Nuclear Fusion, 2017, 57, 036017.	3.5	16
241	Dependence of the turbulent particle flux on hydrogen isotopes induced by collisionality. Physics of Plasmas, 2018, 25, 082517.	1.9	16
242	Review of recent experimental and modeling advances in the understanding of lower hybrid current drive in ITER-relevant regimes. Nuclear Fusion, 2018, 58, 095003.	3.5	16
243	Beam-Ion Acceleration during Edge Localized Modes in the ASDEX Upgrade Tokamak. Physical Review Letters, 2018, 121, 025002.	7.8	16
244	Ionoluminescent response of several phosphor screens to keV ions of different masses. Journal of Applied Physics, 2008, 104, .	2.5	15
245	Quantification of the impact of large and small-scale instabilities on the fast-ion confinement in ASDEX Upgrade. Plasma Physics and Controlled Fusion, 2015, 57, 014018.	2.1	15
246	Bayesian Integrated Data Analysis of Fast-Ion Measurements by Velocity-Space Tomography. Fusion Science and Technology, 2018, 74, 23-36.	1.1	15
247	Fusion product losses due to fishbone instabilities in deuterium JET plasmas. Nuclear Fusion, 2018, 58, 014003.	3.5	15
248	Correlation of surface chemical states with hydrogen isotope retention in divertor tiles of JET with ITER-Like Wall. Fusion Engineering and Design, 2018, 132, 24-28.	1.9	15
249	Fast ion synergistic effects in JET high performance pulses. Nuclear Fusion, 2019, 59, 056005.	3.5	15
250	Optimizing beam-ion confinement in ITER by adjusting the toroidal phase of the 3D magnetic fields applied for ELM control. Nuclear Fusion, 2021, 61, 046006.	3.5	15
251	Deep deuterium retention and Be/W mixing at tungsten coated surfaces in the JET divertor. Physica Scripta, 2016, T167, 014061.	2.5	14
252	How to assess the efficiency of synchronization experiments in tokamaks. Nuclear Fusion, 2016, 56, 076008.	3.5	14

#	Article	IF	CITATIONS
253	Deposition in the inner and outer corners of the JET divertor with carbon wall and metallic ITER-like wall. Physica Scripta, 2016, T167, 014052.	2.5	14
254	Raman microscopy investigation of beryllium materials. Physica Scripta, 2016, T167, 014027.	2.5	14
255	Beryllium film deposition in cavity samples in remote areas of the JET divertor during the 2011–2012 ITER-like wall campaign. Nuclear Materials and Energy, 2017, 12, 548-552.	1.3	14
256	Micro-/nano-characterization of the surface structures on the divertor tiles from JET ITER-like wall. Fusion Engineering and Design, 2017, 116, 1-4.	1.9	14
257	Structure, tritium depth profile and desorption from â€~plasma-facing' beryllium materials of ITER-Like-Wall at JET. Nuclear Materials and Energy, 2017, 12, 642-647.	1.3	14
258	3D simulations of gas puff effects on edge plasma and ICRF coupling in JET. Nuclear Fusion, 2017, 57, 056042.	3.5	14
259	Sub-millisecond electron density profile measurement at the JET tokamak with the fast lithium beam emission spectroscopy system. Review of Scientific Instruments, 2018, 89, 043509.	1.3	14
260	High Z neoclassical transport: Application and limitation of analytical formulae for modelling JET experimental parameters. Physics of Plasmas, 2018, 25, .	1.9	14
261	Pedestal evolution physics in low triangularity JET tokamak discharges with ITER-like wall. Nuclear Fusion, 2018, 58, 016021.	3.5	14
262	On the Use of Transfer Entropy to Investigate the Time Horizon of Causal Influences between Signals. Entropy, 2018, 20, 627.	2.2	14
263	Towards a new image processing system at Wendelstein 7-X: From spatial calibration to characterization of thermal events. Review of Scientific Instruments, 2018, 89, 123503.	1.3	14
264	Real-time protection of the JET ITER-like wall based on near infrared imaging diagnostic systems. Nuclear Fusion, 2018, 58, 106021.	3.5	14
265	Observations and modelling of ion cyclotron emission observed in JET plasmas using a sub-harmonic arc detection system during ion cyclotron resonance heating. Nuclear Fusion, 2018, 58, 096020.	3.5	14
266	Radiation damage and nuclear heating studies in selected functional materials during the JET DT campaign. Fusion Engineering and Design, 2016, 109-111, 1011-1015.	1.9	13
267	High power neon seeded JET discharges: Experiments and simulations. Nuclear Materials and Energy, 2017, 12, 882-886.	1.3	13
268	Temperature response of several scintillator materials to light ions. Nuclear Instruments & Methods in Physics Research B, 2017, 403, 7-12.	1.4	13
269	Comparative H-mode density limit studies in JET and AUG. Nuclear Materials and Energy, 2017, 12, 100-110.	1.3	13
270	Surface composition and structure of divertor tiles following the JET tokamak operation with the ITER-like wall. Nuclear Fusion, 2017, 57, 076027.	3.5	13

#	Article	IF	CITATIONS
271	Deuterium retention in the divertor tiles of JET ITER-Like wall. Nuclear Materials and Energy, 2017, 12, 655-661.	1.3	13
272	Analyses of microstructure, composition and retention of hydrogen isotopes in divertor tiles of JET with the ITER-like wall. Physica Scripta, 2017, T170, 014031.	2.5	13
273	Light impurity transport in JET ILW L-mode plasmas. Nuclear Fusion, 2018, 58, 036009.	3.5	13
274	Determination of 2D poloidal maps of the intrinsic W density for transport studies in JET-ILW. Review of Scientific Instruments, 2018, 89, 113501.	1.3	13
275	Real-time plasma state monitoring and supervisory control on TCV. Nuclear Fusion, 2019, 59, 026017.	3.5	13
276	Gyrokinetic modeling of impurity peaking in JET H-mode plasmas. Physics of Plasmas, 2017, 24, .	1.9	13
277	Fast Sampling Upgrade and Real-Time NTM Control Application of the ECE Radiometer on ASDEX Upgrade. Fusion Science and Technology, 2010, 57, 1-9.	1.1	12
278	Numerical simulation of fast ion loss detector measurements for fishbones on JET. Nuclear Fusion, 2011, 51, 053003.	3.5	12
279	Trapped electron mode driven electron heat transport in JET: experimental investigation and gyro-kinetic theory validation. Nuclear Fusion, 2015, 55, 113016.	3.5	12
280	Diagnostic application of magnetic islands rotation in JET. Nuclear Fusion, 2016, 56, 076004.	3.5	12
281	Studies of Be migration in the JET tokamak using AMS with 10Be marker. Nuclear Instruments & Methods in Physics Research B, 2016, 371, 370-375.	1.4	12
282	Calculations to support JET neutron yield calibration: Modelling of neutron emission from a compact DT neutron generator. Nuclear Instruments and Methods in Physics Research, Section A: Accelerators, Spectrometers, Detectors and Associated Equipment, 2017, 847, 199-204.	1.6	12
283	Charge collection uniformity and irradiation effects of synthetic diamond detectors studied with a proton micro-beam. Nuclear Instruments & Methods in Physics Research B, 2017, 405, 1-10.	1.4	12
284	A tool to support the construction of reliable disruption databases. Fusion Engineering and Design, 2017, 125, 139-153.	1.9	12
285	First absolute measurements of fast-ion losses in the ASDEX Upgrade tokamak. Plasma Physics and Controlled Fusion, 2017, 59, 105009.	2.1	12
286	Erosion at the inner wall of JET during the discharge campaign 2013–2014. Nuclear Materials and Energy, 2017, 11, 20-24.	1.3	12
287	Assessment of divertor heat load with and without external magnetic perturbation. Nuclear Fusion, 2017, 57, 066045.	3.5	12
288	Metallic mirrors for plasma diagnosis in current and future reactors: tests for ITER and DEMO. Physica Scripta, 2017, T170, 014061.	2.5	12

#	Article	IF	CITATIONS
289	Equilibrium reconstruction in an iron core tokamak using a deterministic magnetisation model. Computer Physics Communications, 2018, 223, 1-17.	7.5	12
290	Comparison of runaway electron generation parameters in small, medium-sized and large tokamaks—A survey of experiments in COMPASS, TCV, ASDEX-Upgrade and JET. Nuclear Fusion, 2018, 58, 016014.	3.5	12
291	Assessment of the strength of kinetic effects of parallel electron transport in the SOL and divertor of JET high radiative H-mode plasmas using EDGE2D-EIRENE and KIPP codes. Plasma Physics and Controlled Fusion, 2018, 60, 115011.	2.1	12
292	Development of a new compact gamma-ray spectrometer optimised for runaway electron measurements. Review of Scientific Instruments, 2018, 89, 101134.	1.3	12
293	First measurements of a scintillator based fast-ion loss detector near the ASDEX Upgrade divertor. Review of Scientific Instruments, 2018, 89, 101106.	1.3	12
294	Core plasma ion cyclotron emission driven by fusion-born ions. Nuclear Fusion, 2019, 59, 014001.	3.5	12
295	Observation of Alfvén Eigenmodes driven by off-axis neutral beam injection in the TCV tokamak. Plasma Physics and Controlled Fusion, 2020, 62, 095017.	2.1	12
296	TAE internal structure through high-resolution soft x-ray measurements in ASDEX-Upgrade. Nuclear Fusion, 2008, 48, 065001.	3.5	11
297	Overview of ASDEX Upgrade results. Nuclear Fusion, 2009, 49, 104009.	3.5	11
298	Impact of strongly driven fishbones and Alfvén Eigenmodes on fast ion losses. Nuclear Fusion, 2010, 50, 115006.	3.5	11
299	Characterization of scintillator materials for fast-ion loss detectors in nuclear fusion reactors. Nuclear Instruments & Methods in Physics Research B, 2014, 332, 216-219.	1.4	11
300	On the interpretation of high-resolution x-ray spectra from JET with an ITER-like wall. Journal of Physics B: Atomic, Molecular and Optical Physics, 2015, 48, 144028.	1.5	11
301	Progress in reducing ICRF-specific impurity release in ASDEX upgrade and JET. Nuclear Materials and Energy, 2017, 12, 1194-1198.	1.3	11
302	Upgrade of the tangential gamma-ray spectrometer beam-line for JET DT experiments. Fusion Engineering and Design, 2017, 123, 749-753.	1.9	11
303	Numerical analysis of ELM stability with rotation and ion diamagnetic drift effects in JET. Nuclear Fusion, 2017, 57, 126001.	3.5	11
304	Activation measurements in support of the 14 MeV neutron calibration of JET neutron monitors. Fusion Engineering and Design, 2017, 125, 50-56.	1.9	11
305	Statistical validation of predictive TRANSP simulations of baseline discharges in preparation for extrapolation to JET D–T. Nuclear Fusion, 2017, 57, 066032.	3.5	11
306	Comparison of JET AVDE disruption data with M3D simulations and implications for ITER. Physics of Plasmas, 2017, 24, .	1.9	11

#	Article	IF	CITATIONS
307	TAE stability calculations compared to TAE antenna results in JET. Nuclear Fusion, 2018, 58, 082007.	3.5	11
308	A rotary and reciprocating scintillator based fast-ion loss detector for the MAST-U tokamak. Review of Scientific Instruments, 2018, 89, 10I112.	1.3	11
309	Long-lived coupled peeling ballooning modes preceding ELMs on JET. Nuclear Fusion, 2019, 59, 056004.	3.5	11
310	Characterization of Alfvén eigenmodes using NBI during current ramp-up in the ASDEX Upgrade tokamak. Plasma Physics and Controlled Fusion, 2012, 54, 095014.	2.1	10
311	Scrape-off layer ion acceleration during fast wave injection in the DIII-D tokamak. Nuclear Fusion, 2012, 52, 063019.	3.5	10
312	Fusion alpha-particle diagnostics for DT experiments on the joint European torus. AIP Conference Proceedings, 2014, , .	0.4	10
313	An FPGA-based bolometer for the MAST-U Super-X divertor. Review of Scientific Instruments, 2016, 87, 11E721.	1.3	10
314	Bayesian modelling of the emission spectrum of the Joint European Torus Lithium Beam Emission Spectroscopy system. Review of Scientific Instruments, 2016, 87, 023501.	1.3	10
315	Extending helium partial pressure measurement technology to JET DTE2 and ITER. Review of Scientific Instruments, 2016, 87, 11D442.	1.3	10
316	Advanced design of the Mechanical Tritium Pumping System for JET DTE2. Fusion Engineering and Design, 2016, 109-111, 359-364.	1.9	10
317	Tritium distributions on tungsten and carbon tiles used in the JET divertor. Physica Scripta, 2016, T167, 014009.	2.5	10
318	In situ wavelength calibration of the edge CXS spectrometers on JET. Review of Scientific Instruments, 2016, 87, 11E525.	1.3	10
319	Technical preparations for the in-vessel 14 MeV neutron calibration at JET. Fusion Engineering and Design, 2017, 117, 107-114.	1.9	10
320	Status of ITER material activation experiments at JET. Fusion Engineering and Design, 2017, 124, 1150-1155.	1.9	10
321	On efficiency and interpretation of sawteeth pacing with on-axis ICRH modulation in JET. Nuclear Fusion, 2017, 57, 126057.	3.5	10
322	Simulation of JET ITER-Like Wall pulses at high neon seeding rate. Nuclear Fusion, 2017, 57, 126021.	3.5	10
323	The isotope effect on divertor conditions and neutral pumping in horizontal divertor configurations in JET-ILW Ohmic plasmas. Nuclear Materials and Energy, 2017, 12, 791-797.	1.3	10
324	An analytical expression for ion velocities at the wall including the sheath electric field and surface biasing for erosion modeling at JET ILW. Nuclear Materials and Energy, 2017, 12, 341-345.	1.3	10

#	Article	IF	CITATIONS
325	On the potential of ruled-based machine learning for disruption prediction on JET. Fusion Engineering and Design, 2018, 130, 62-68.	1.9	10
326	Tritium distributions on W-coated divertor tiles used in the third JET ITER-like wall campaign. Nuclear Materials and Energy, 2019, 18, 258-261.	1.3	10
327	Beam modulation and bump-on-tail effects on Alfvén eigenmode stability in DIII-D. Nuclear Fusion, 2021, 61, 066028.	3.5	10
328	Coils and power supplies design for the SMART tokamak. Fusion Engineering and Design, 2021, 168, 112683.	1.9	10
329	Transport of energetic ions due to sawteeth, Alfvén eigenmodes and microturbulence. Nuclear Fusion, 2011, 51, 043012.	3.5	9
330	Study of the triton-burnup process in different JET scenarios using neutron monitor based on CVD diamond. Review of Scientific Instruments, 2016, 87, 11D835.	1.3	9
331	JET diagnostic enhancements in preparation for DT operations. Review of Scientific Instruments, 2016, 87, 11D443.	1.3	9
332	Hardware architecture of the data acquisition and processing system for the JET Neutron Camera Upgrade (NCU) project. Fusion Engineering and Design, 2017, 123, 873-876.	1.9	9
333	The effect of the isotope on the H-mode density limit. Nuclear Fusion, 2017, 57, 086007.	3.5	9
334	The emissivity of W coatings deposited on carbon materials for fusion applications. Fusion Engineering and Design, 2017, 114, 192-195.	1.9	9
335	Response of the imaging cameras to hard radiation during JET operation. Fusion Engineering and Design, 2017, 123, 669-673.	1.9	9
336	Conceptual design of a scintillator based Imaging Heavy Ion Beam Probe for the ASDEX Upgrade tokamak. Journal of Instrumentation, 2017, 12, C08023-C08023.	1.2	9
337	ERO modeling and sensitivity analysis of locally enhanced beryllium erosion by magnetically connected antennas. Nuclear Fusion, 2018, 58, 016046.	3.5	9
338	Modelling of the neutron production in a mixed beam DT neutron generator. Fusion Engineering and Design, 2018, 136, 1089-1093.	1.9	9
339	Generation of a plasma neutron source for Monte Carlo neutron transport calculations in the tokamak JET. Fusion Engineering and Design, 2018, 136, 1047-1051.	1.9	9
340	Analysis of plasma termination in the JET hybrid scenario. Nuclear Fusion, 2018, 58, 076027.	3.5	9
341	Full-orbit and drift calculations of fusion product losses due to explosive fishbones on JET. Nuclear Fusion, 2019, 59, 016004.	3.5	9
342	Mechanical and electromagnetic design of the vacuum vessel of the SMART tokamak. Fusion Engineering and Design, 2021, 171, 112542.	1.9	9

#	Article	IF	CITATIONS
343	Plasma isotopic changeover experiments in JET under carbon and ITER-like wall conditions. Nuclear Fusion, 2015, 55, 043021.	3.5	8
344	A fast feedback controlled magnetic drive for the ASDEX Upgrade fast-ion loss detectors. Review of Scientific Instruments, 2016, 87, 11E705.	1.3	8
345	Characterization of a diamond detector to be used as neutron yield monitor during the in-vessel calibration of JET neutron detectors in preparation of the DT experiment. Fusion Engineering and Design, 2016, 106, 93-98.	1.9	8
346	On the mechanisms governing gas penetration into a tokamak plasma during a massive gas injection. Nuclear Fusion, 2017, 57, 016027.	3.5	8
347	The near infrared imaging system for the real-time protection of the JET ITER-like wall. Physica Scripta, 2017, T170, 014027.	2.5	8
348	Characterization of a compact LaBr ₃ (Ce) detector with Silicon photomultipliers at high 14 MeV neutron fluxes. Journal of Instrumentation, 2017, 12, C10007-C10007.	1.2	8
349	Analysis of possible improvement of the plasma performance in JET due to the inward spatial channelling of fast-ion energy. Nuclear Fusion, 2018, 58, 076012.	3.5	8
350	On the universality of power laws for tokamak plasma predictions. Plasma Physics and Controlled Fusion, 2018, 60, 025028.	2.1	8
351	On the role of finite grid extent in SOLPS-ITER edge plasma simulations for JET H-mode discharges with metallic wall. Nuclear Materials and Energy, 2018, 17, 174-181.	1.3	8
352	Neutron emission spectroscopy of D plasmas at JET with a compact liquid scintillating neutron spectrometer. Review of Scientific Instruments, 2018, 89, 101113.	1.3	8
353	A locked mode indicator for disruption prediction on JET and ASDEX upgrade. Fusion Engineering and Design, 2019, 138, 254-266.	1.9	8
354	IBIC analysis of SiC detectors developed for fusion applications. Radiation Physics and Chemistry, 2020, 177, 109100.	2.8	8
355	Turbulent transport analysis of JET H-mode and hybrid plasmas using QuaLiKiz and Trapped Gyro Landau Fluid. Plasma Physics and Controlled Fusion, 2015, 57, 035003.	2.1	7
356	Edge profile analysis of Joint European Torus (JET) Thomson scattering data: Quantifying the systematic error due to edge localised mode synchronisation. Review of Scientific Instruments, 2016, 87, 013507.	1.3	7
357	Upgrades of Diagnostic Techniques and Technologies for JET Next D-T Campaigns. IEEE Transactions on Nuclear Science, 2016, 63, 1674-1681.	2.0	7
358	Comparison of dust transport modelling codes in a tokamak plasma. Physics of Plasmas, 2016, 23, 102506.	1.9	7
359	Real-time control of ELM and sawtooth frequencies: similarities and differences. Nuclear Fusion, 2016, 56, 016008.	3.5	7
360	JET experience on managing radioactive waste and implications for ITER. Fusion Engineering and Design, 2016, 109-111, 979-985.	1.9	7

#	Article	IF	CITATIONS
361	Advances in understanding and utilising ELM control in JET. Plasma Physics and Controlled Fusion, 2016, 58, 014017.	2.1	7
362	Commissioning and first results of the reinstated JET ICRF ILA. Fusion Engineering and Design, 2017, 123, 285-288.	1.9	7
363	The preparation of the Shutdown Dose Rate experiment for the next JET Deuterium-Tritium campaign. Fusion Engineering and Design, 2017, 123, 1039-1043.	1.9	7
364	Expanding the role of impurity spectroscopy for investigating the physics of high-Z dissipative divertors. Nuclear Materials and Energy, 2017, 12, 91-99.	1.3	7
365	Main chamber wall plasma loads in JET-ITER-like wall at high radiated fraction. Nuclear Materials and Energy, 2017, 12, 234-240.	1.3	7
366	Real time control developments at JET in preparation for deuterium-tritium operation. Fusion Engineering and Design, 2017, 123, 535-540.	1.9	7
367	Synthetic neutron camera and spectrometer in JET based on AFSI-ASCOT simulations. Journal of Instrumentation, 2017, 12, C09010-C09010.	1.2	7
368	Detection of Causal Relations in Time Series Affected by Noise in Tokamaks Using Geodesic Distance on Gaussian Manifolds. Entropy, 2017, 19, 569.	2.2	7
369	Testing of tritium breeder blanket activation foil spectrometer during JET operations. Fusion Engineering and Design, 2018, 136, 258-264.	1.9	7
370	MHD spectroscopy of JET plasmas with pellets via Alfvén eigenmodes. Nuclear Fusion, 2018, 58, 082008.	3.5	7
371	JET diagnostic enhancements testing and commissioning in preparation for DT scientific campaigns. Review of Scientific Instruments, 2018, 89, 10K119.	1.3	7
372	Synthesis of Chiral 1,3-Dienes through Ring-Closing Metathesis of Enantioenriched Enynes: Potential Precursors of Morphane Analogs. Anais Da Academia Brasileira De Ciencias, 2018, 90, 1059-1072.	0.8	7
373	Molecular ND Band Spectroscopy in the Divertor Region of Nitrogen Seeded JET Discharges. Journal of Physics: Conference Series, 2018, 959, 012009.	0.4	7
374	TLD calibration for neutron fluence measurements at JET fusion facility. Nuclear Instruments and Methods in Physics Research, Section A: Accelerators, Spectrometers, Detectors and Associated Equipment, 2018, 904, 202-213.	1.6	7
375	Observation of accelerated beam ion population during edge localized modes in the ASDEX Upgrade tokamak. Nuclear Fusion, 2019, 59, 066016.	3.5	7
376	Gyrokinetic simulations of toroidal Alfvén eigenmodes excited by energetic ions and external antennas on the Joint European Torus. Nuclear Fusion, 2019, 59, 026008.	3.5	7
377	Improved neutron activation dosimetry for fusion. Fusion Engineering and Design, 2019, 139, 109-114.	1.9	7
378	Design and simulation of an imaging neutral particle analyzer for the ASDEX Upgrade tokamak. Review of Scientific Instruments, 2021, 92, 043554.	1.3	7

#	Article	IF	CITATIONS
379	Stability of toroidicity induced shear Alfvén eigenmodes in ASDEX Upgrade. Plasma Physics and Controlled Fusion, 2009, 51, 065003.	2.1	6
380	ICRH beatwave excited toroidicity induced Alfvén eigenmodes in ASDEX Upgrade. Nuclear Fusion, 2010, 50, 052003.	3.5	6
381	Comparative analysis of core heat transport of JET high density H-mode plasmas in carbon wall and ITER-like wall. Plasma Physics and Controlled Fusion, 2015, 57, 065002.	2.1	6
382	Integrated core–SOL–divertor modelling for ITER including impurity: effect of tungsten on fusion performance in H-mode and hybrid scenario. Nuclear Fusion, 2015, 55, 053032.	3.5	6
383	Simulating the nitrogen migration in Be/W tokamaks with WallDYN. Physica Scripta, 2016, T167, 014079.	2.5	6
384	ITER-like antenna capacitors voltage probes: Circuit/electromagnetic calculations and calibrations. Review of Scientific Instruments, 2016, 87, 104705.	1.3	6
385	Sparse representation of signals: from astrophysics to real-time data analysis for fusion plasmas and system optimization analysis for ITER and TCV. Plasma Physics and Controlled Fusion, 2016, 58, 123001.	2.1	6
386	Evaluation of reconstruction errors and identification of artefacts for JET gamma and neutron tomography. Review of Scientific Instruments, 2016, 87, 013502.	1.3	6
387	COREDIV and SOLPS Numerical Simulations of the Nitrogen Seeded JET ILW Lâ€mode Discharges. Contributions To Plasma Physics, 2016, 56, 760-765.	1.1	6
388	Effect of PFC Recycling Conditions on JET Pedestal Density. Contributions To Plasma Physics, 2016, 56, 754-759.	1.1	6
389	Global optimization driven by genetic algorithms for disruption predictors based on APODIS architecture. Fusion Engineering and Design, 2016, 112, 1014-1018.	1.9	6
390	Investigation on the erosion/deposition processes in the ITER-like wall divertor at JET using glow discharge optical emission spectrometry technique. Physica Scripta, 2016, T167, 014049.	2.5	6
391	Impact of the JET ITER-like wall on H-mode plasma fueling. Nuclear Fusion, 2017, 57, 066024.	3.5	6
392	The effect of lower hybrid waves on JET plasma rotation. Nuclear Fusion, 2017, 57, 034002.	3.5	6
393	Evaluation of the plasma hydrogen isotope content by residual gas analysis at JET and AUG. Physica Scripta, 2017, T170, 014021.	2.5	6
394	Quartz micro-balance results of pulse-resolved erosion/deposition in the JET-ILW divertor. Nuclear Materials and Energy, 2017, 12, 478-482.	1.3	6
395	Analysis of activation and damage of ITER material samples expected from DD/DT campaign at JET. Fusion Engineering and Design, 2017, 125, 307-313.	1.9	6
396	Impurity re-distribution in the corner regions of the JET divertor. Physica Scripta, 2017, T170, 014060.	2.5	6

#	Article	IF	CITATIONS
397	Self-consistent coupling of DSMC method and SOLPS code for modeling tokamak particle exhaust. Nuclear Fusion, 2017, 57, 066037.	3.5	6
398	An improved model for the accurate calculation of parallel heat fluxes at the JET bulk tungsten outer divertor. Nuclear Fusion, 2018, 58, 106034.	3.5	6
399	Forward modeling of collective Thomson scattering for Wendelstein 7-X plasmas: Electrostatic approximation. Review of Scientific Instruments, 2019, 90, 023501.	1.3	6
400	First measurements of a magnetically driven fast-ion loss detector on ASDEX Upgrade. Journal of Instrumentation, 2019, 14, C11005-C11005.	1.2	6
401	ELM-induced cold pulse propagation in ASDEX Upgrade. Plasma Physics and Controlled Fusion, 2019, 61, 045003.	2.1	6
402	Upgrade and absolute calibration of the JET scintillator-based fast-ion loss detector. Review of Scientific Instruments, 2021, 92, 043553.	1.3	6
403	Tritium analysis of divertor tiles used in JET ITER-like wall campaigns by means of <i>β</i> -ray induced x-ray spectrometry. Physica Scripta, 2017, T170, 014014.	2.5	6
404	Time-resolved deposition in the remote region of the JET-ILW divertor: measurements and modelling. Physica Scripta, 2017, T170, 014059.	2.5	6
405	Plasma physics and control studies planned in JT-60SA for ITER and DEMO operations and risk mitigation. Plasma Physics and Controlled Fusion, 2022, 64, 054004.	2.1	6
406	Identification of geodesic chirping Alfvén modes and <i>q</i> -factor estimation in hot core tokamak plasmas in ASDEX Upgrade. Plasma Physics and Controlled Fusion, 2011, 53, 025006.	2.1	5
407	Feasibility Study of Lost-Alpha-Particle Measurements by Probe Technique in ITER. Fusion Science and Technology, 2012, 61, 172-184.	1.1	5
408	Bernstein polynomial and discontinuous functions. Journal of Mathematical Analysis and Applications, 2014, 411, 829-837.	1.0	5
409	The merits of ion cyclotron resonance heating schemes for sawtooth control in tokamak plasmas. Journal of Plasma Physics, 2015, 81, .	2.1	5
410	Core fusion power gain and alpha heating in JET, TFTR, and ITER. Nuclear Fusion, 2016, 56, 056002.	3.5	5
411	Neutronic analysis of JET external neutron monitor response. Fusion Engineering and Design, 2016, 109-111, 99-103.	1.9	5
412	The non-thermal origin of the tokamak low-density stability limit. Nuclear Fusion, 2016, 56, 056010.	3.5	5
413	Plasma turbulence measured with fast frequency swept reflectometry in JET H-mode plasmas. Nuclear Fusion, 2016, 56, 126019.	3.5	5
414	Hybrid cancellation of ripple disturbances arising in AC/DC converters. Automatica, 2017, 77, 344-352.	5.0	5

#	Article	IF	CITATIONS
415	Generation of the neutron response function of an NE213 scintillator for fusion applications. Nuclear Instruments and Methods in Physics Research, Section A: Accelerators, Spectrometers, Detectors and Associated Equipment, 2017, 866, 222-229.	1.6	5
416	Development of MPPC-based detectors for high count rate DT campaigns at JET. Fusion Engineering and Design, 2017, 123, 940-944.	1.9	5
417	Characterisation of neutron generators and monitoring detectors for the in-vessel calibration of JET. Fusion Engineering and Design, 2018, 136, 233-238.	1.9	5
418	Plasma-wall interaction on the divertor tiles of JET ITER-like wall from the viewpoint of micro/nanoscopic observations. Fusion Engineering and Design, 2018, 136, 199-204.	1.9	5
419	ICRH antennaS-matrix measurements and plasma coupling characterisation at JET. Nuclear Fusion, 2018, 58, 046012.	3.5	5
420	Shutdown dose rate measurements after the 2016 Deuterium-Deuterium campaign at JET. Fusion Engineering and Design, 2018, 136, 1348-1353.	1.9	5
421	Application of the Denovo Discrete Ordinates Radiation Transport Code to Large-Scale Fusion Neutronics. Fusion Science and Technology, 2018, 74, 303-314.	1.1	5
422	Shutdown dose rate neutronics experiment during high performances DD operations at JET. Fusion Engineering and Design, 2018, 136, 1545-1549.	1.9	5
423	Preparation for commissioning of materials detritiation facility at Culham Science Centre. Fusion Engineering and Design, 2018, 136, 1391-1395.	1.9	5
424	Scaling of the geodesic acoustic mode amplitude on JET. Plasma Physics and Controlled Fusion, 2018, 60, 085006.	2.1	5
425	Approximate analytic expressions using Stokes model for tokamak polarimetry and their range of validity. Plasma Physics and Controlled Fusion, 2019, 61, 055008.	2.1	5
426	Magnetic equilibrium design for the SMART tokamak. Fusion Engineering and Design, 2021, 171, 112706.	1.9	5
427	Experimental investigation of the confinement of d(³ He,p) <i>α</i> and d(d,p)t fusion reaction products in JET. Nuclear Fusion, 2012, 52, 083004.	3.5	4
428	The global build-up to intrinsic edge localized mode bursts seen in divertor full flux loops in JET. Physics of Plasmas, 2015, 22, .	1.9	4
429	Conceptual Design of the Mechanical Tritium Pumping System for JET DTE2. Fusion Science and Technology, 2015, 68, 630-634.	1.1	4
430	Scaling of the frequencies of the type one edge localized modes and their effect on the tungsten source in JET ITER-like wall. Plasma Physics and Controlled Fusion, 2016, 58, 125014.	2.1	4
431	A prototype fully digital data acquisition system upgrade for the TOFOR neutron spectrometer at JET. Nuclear Instruments and Methods in Physics Research, Section A: Accelerators, Spectrometers, Detectors and Associated Equipment, 2016, 833, 94-104.	1.6	4
432	Stabilization of sawteeth with third harmonic deuterium ICRF-accelerated beam in JET plasmas. Physics of Plasmas, 2016, 23, 012505.	1.9	4

#	Article	IF	CITATIONS
433	Risk Mitigation for ITER by a Prolonged and Joint International Operation of JET. Journal of Fusion Energy, 2016, 35, 85-93.	1.2	4
434	Calculation of the profile-dependent neutron backscatter matrix for the JET neutron camera system. Fusion Engineering and Design, 2017, 123, 865-868.	1.9	4
435	CeBr3–based detector for gamma-ray spectrometer upgrade at JET. Fusion Engineering and Design, 2017, 123, 986-989.	1.9	4
436	Determining the prediction limits of models and classifiers with applications for disruption prediction in JET. Nuclear Fusion, 2017, 57, 016024.	3.5	4
437	Be ITER-like wall at the JET tokamak under plasma. Physica Scripta, 2017, T170, 014049.	2.5	4
438	Synthetic NPA diagnostic for energetic particles in JET plasmas. Journal of Instrumentation, 2017, 12, C11025-C11025.	1.2	4
439	Control and data acquisition software upgrade for JET gamma-ray diagnostics. Fusion Engineering and Design, 2018, 128, 117-121.	1.9	4
440	Application of the VUV and the soft x-ray systems on JET for the study of intrinsic impurity behavior in neon seeded hybrid discharges. Review of Scientific Instruments, 2018, 89, 10D131.	1.3	4
441	Inter-ELM evolution of the edge current density in JET-ILW type I ELMy H-mode plasmas. Plasma Physics and Controlled Fusion, 2018, 60, 085003.	2.1	4
442	On a fusion born triton effect in JET deuterium discharges with H-minority ion cyclotron range of frequencies heating. Nuclear Fusion, 2019, 59, 064001.	3.5	4
443	Beam modelling and hardware design of an imaging heavy ion beam probe for ASDEX Upgrade. Journal of Instrumentation, 2019, 14, C10030-C10030.	1.2	4
444	Thermo-mechanical assessment of the JT-60SA fast-ion loss detector. Fusion Engineering and Design, 2021, 167, 112304.	1.9	4
445	Characterization of scintillator screens for suprathermal ion detection in fusion devices. Journal of Instrumentation, 2011, 6, P04002-P04002.	1.2	3
446	Robust regression with CUDA and its application to plasma reflectometry. Review of Scientific Instruments, 2015, 86, 113507.	1.3	3
447	Free boundary equilibrium in 3D tokamaks with toroidal rotation. Nuclear Fusion, 2015, 55, 063032.	3.5	3
448	Comparative gyrokinetic analysis of JET baseline H-mode core plasmas with carbon wall and ITER-like wall. Plasma Physics and Controlled Fusion, 2016, 58, 045021.	2.1	3
449	A classification scheme for edge-localized modes based on their probability distributions. Review of Scientific Instruments, 2016, 87, 11D404.	1.3	3
450	Numerical calculations of non-inductive current driven by microwaves in JET. Plasma Physics and Controlled Fusion, 2016, 58, 125001.	2.1	3

#	Article	IF	CITATIONS
451	JET Tokamak, preparation of a safety case for tritium operations. Fusion Engineering and Design, 2016, 109-111, 1308-1312.	1.9	3
452	Kinematic background discrimination methods using a fully digital data acquisition system for TOFOR. Nuclear Instruments and Methods in Physics Research, Section A: Accelerators, Spectrometers, Detectors and Associated Equipment, 2016, 838, 82-88.	1.6	3
453	Modelling of the JET DT Experiments in Carbon and ITER-like Wall Configurations. Contributions To Plasma Physics, 2016, 56, 766-771.	1.1	3
454	Correlation analysis for energy losses, waiting times and durations of type I edge-localized modes in the Joint European Torus. Nuclear Fusion, 2017, 57, 036026.	3.5	3
455	The global build-up to intrinsic ELM bursts and comparison with pellet triggered ELMs seen in JET. Nuclear Fusion, 2017, 57, 022017.	3.5	3
456	A 3D electromagnetic model of the iron core in JET. Fusion Engineering and Design, 2017, 123, 527-531.	1.9	3
457	Dynamic and thermal simulations of a fast-ion loss detector for ITER. Fusion Engineering and Design, 2017, 123, 807-810.	1.9	3
458	EDGE2D-EIRENE simulations of the impact of poloidal flux expansion on the radiative divertor performance in JET. Nuclear Materials and Energy, 2017, 12, 786-790.	1.3	3
459	Intra-ELM tungsten sputtering in JET ITER-like wall: analytical studies of Be impurity and ELM type influence. Physica Scripta, 2017, T170, 014065.	2.5	3
460	Evidence of9Be  +  pnuclear reactions during 2ωCHand hydrogen minority ICRH in JET-ILW h deuterium plasmas. Nuclear Fusion, 2018, 58, 026033.	ydrogen a	nd ₃
461	Escaping alpha-particle monitor for burning plasmas. Nuclear Fusion, 2018, 58, 082009.	3.5	3
462	Nonlinear dynamic analysis of Dαsignals for type I edge localized modes characterization on JET with a carbon wall. Plasma Physics and Controlled Fusion, 2018, 60, 025010.	2.1	3
463	Heat flux analysis of Type-I ELM impact on a sloped, protruding surface in the JET bulk tungsten divertor. Nuclear Materials and Energy, 2018, 17, 182-187.	1.3	3
464	Activation material selection for multiple foil activation detectors in JET TT campaign. Fusion Engineering and Design, 2018, 136, 988-992.	1.9	3
465	Alpha heating, isotopic mass, and fast ion effects in deuterium–tritium experiments. Nuclear Fusion, 2018, 58, 096011.	3.5	3
466	A fast model to resolve the velocity-space of fast-ion losses detected in ASDEX Upgrade and MAST Upgrade. Journal of Instrumentation, 2019, 14, C09015-C09015.	1.2	3
467	Radial variation of heat transport in L-mode JET discharges. Nuclear Fusion, 2019, 59, 056006.	3.5	3
468	Upgrade of the edge Charge Exchange Recombination Spectroscopy system at the High Field Side of ASDEX Upgrade. Journal of Instrumentation, 2019, 14, C11006-C11006.	1.2	3

#	Article	IF	CITATIONS
469	Analysis of the outer divertor hot spot activity in the protection video camera recordings at JET. Fusion Engineering and Design, 2019, 139, 115-123.	1.9	3
470	Self-adaptive diagnostic of radial fast-ion loss measurements on the ASDEX Upgrade tokamak (invited). Review of Scientific Instruments, 2021, 92, 053538.	1.3	3
471	Postnikov invariants of crossed complexes. Journal of Algebra, 2005, 285, 238-291.	0.7	2
472	Nonlinear alfvénic fast particle transport and losses. Journal of Physics: Conference Series, 2012, 401, 012022.	0.4	2
473	Studies of the non-axisymmetric plasma boundary displacement in JET in presence of externally applied magnetic field. Plasma Physics and Controlled Fusion, 2015, 57, 104003.	2.1	2
474	Ion temperature and toroidal rotation in JET's low torque plasmas. Review of Scientific Instruments, 2016, 87, 11E557.	1.3	2
475	A generalized Abel inversion method for gamma-ray imaging of thermonuclear plasmas. Journal of Instrumentation, 2016, 11, C03001-C03001.	1.2	2
476	Thermo-mechanical properties of W/Mo markers coatings deposited on bulk W. Physica Scripta, 2016, T167, 014028.	2.5	2
477	Modelling of plasma-edge and plasma–wall interaction physics at JET with the metallic first-wall. Physica Scripta, 2016, T167, 014078.	2.5	2
478	Towards self-consistent plasma modelisation in presence of neoclassical tearing mode and sawteeth: effects on transport coefficients. Plasma Physics and Controlled Fusion, 2017, 59, 125012.	2.1	2
479	Gyrokinetic simulations of particle transport in pellet fuelled JET discharges. Plasma Physics and Controlled Fusion, 2017, 59, 105005.	2.1	2
480	Dynamic power balance analysis in JET. Physica Scripta, 2017, T170, 014035.	2.5	2
481	Real-time implementation with FPGA-based DAQ system of a probabilistic disruption predictor from scratch. Fusion Engineering and Design, 2018, 129, 179-182.	1.9	2
482	Feasibility study for an edge main ion charge exchange recombination spectroscopy system at ASDEX Upgrade. Journal of Instrumentation, 2019, 14, C10040-C10040.	1.2	2
483	Nonlinear trapping in the bounce-transit and drift resonance and neoclassical toroidal plasma viscosity in tokamaks. Nuclear Fusion, 2020, 60, 056002.	3.5	2
484	Implementation of synthetic fast-ion loss detector and imaging heavy ion beam probe diagnostics in the 3D hybrid kinetic-MHD code MEGA. Review of Scientific Instruments, 2021, 92, 043558.	1.3	2
485	Single and double null equilibria in the SMART Tokamak. Plasma Research Express, 2021, 3, 044001.	0.9	2
486	Thermo-mechanical limits of a magnetically driven fast-ion loss detector in the ASDEX Upgrade tokamak. Journal of Instrumentation, 2022, 17, C02020.	1.2	2

#	Article	IF	CITATIONS
487	Characterization of scintillator screens under irradiation of low energy ¹³³ Cs ions. Journal of Instrumentation, 2022, 17, P02026.	1.2	2
488	In-out charge exchange measurements and 3D modelling of diagnostic thermal neutrals to study edge poloidal impurity asymmetries. Plasma Physics and Controlled Fusion, 2022, 64, 045021.	2.1	2
489	Analysis of ICRF-Accelerated Ions in ASDEX Upgrade. AIP Conference Proceedings, 2007, , .	0.4	1
490	X-ray micro-laminography for the <i>ex situ</i> analysis of W-CFC samples retrieved from JET ITER-like wall. Physica Scripta, 2016, T167, 014050.	2.5	1
491	Thermal analysis of protruding surfaces in the JET divertor. Nuclear Fusion, 2017, 57, 066009.	3.5	1
492	Classification of ELM types in Joint European Torus based on global plasma parameters using discriminant analysis. Fusion Engineering and Design, 2017, 123, 717-721.	1.9	1
493	The impact of the fast ion fluxes and thermal plasma loads on the design of the ITER fast ion loss detector. Journal of Instrumentation, 2017, 12, C12027-C12027.	1.2	1
494	Divertor currents optimization procedure for JET-ILW high flux expansion experiments. Fusion Engineering and Design, 2018, 129, 115-119.	1.9	1
495	Modelling of JET DT experiments in ILW configurations. Contributions To Plasma Physics, 2018, 58, 739-745.	1.1	1
496	Population modelling of the He II energy levels in tokamak plasmas: I. Collisional excitation model. Journal of Physics B: Atomic, Molecular and Optical Physics, 2019, 52, 045001.	1.5	1
497	Nonlinear trapping in wave–particle interactions in tokamaks. Nuclear Fusion, 2021, 61, 046009.	3.5	1
498	Hardware developments and commissioning of the imaging heavy ion beam probe at ASDEX upgrade. Fusion Engineering and Design, 2021, 168, 112644.	1.9	1
499	On determining the prediction limits of mathematical models for time series. Journal of Instrumentation, 2016, 11, C07013-C07013.	1.2	1
500	Fast-ion transport and toroidal rotation response to externally applied magnetic perturbations at the ASDEX Upgrade tokamak. Nuclear Fusion, 0, , .	3.5	1
501	Energetic particle acceleration and transport by Alfvén/acoustic waves in tokamak-like Solar flares. Proceedings of the International Astronomical Union, 2010, 6, 162-164.	0.0	0
502	Addendum to papers from Axially Symmetric Divertor Experiment (ASDEX) Upgrade Team, published in Review of Scientific Instruments. Review of Scientific Instruments, 2010, 81, 039903.	1.3	0
503	Classification of JET Neutron and Gamma Emissivity Profiles. Journal of Instrumentation, 2016, 11, C05021-C05021.	1.2	0
504	MHD marking using the MSE polarimeter optics in ILW JET plasmas. Review of Scientific Instruments, 2016, 87, 11F556.	1.3	0

#	Article	IF	CITATIONS
505	Characteristics of pre-ELM structures during ELM control experiment on JET withn  =  2 magnet perturbations. Nuclear Fusion, 2016, 56, 092011.	ic _{3.5}	0
506	First observation of the depolarization of Thomson scattering radiation by a fusion plasma. Nuclear Fusion, 2018, 58, 044003.	3.5	0
507	Propagating transport-code input parameter uncertainties with deterministic sampling. Plasma Physics and Controlled Fusion, 2018, 60, 125010.	2.1	0
508	Determination of the Fast-Ion Phase-Space Coverage for the FILD Spatial Array of the ASDEX Upgrade Tokamak. Journal of Instrumentation, 2019, 14, C10032-C10032.	1.2	0
509	Characterization of the response of Fast Ion Loss Detectors to fusion neutrons for applications at JT-60SA and ITER. Fusion Engineering and Design, 2021, 173, 112913.	1.9	0
510	Conceptual Design of a Scintillator-Based Fast-Ion Loss Detector for the Wendelstein 7-X Stellarator. IEEE Transactions on Plasma Science, 2022, , 1-0.	1.3	0